

Article

Antibacterial Properties of Zn Doped Hydrophobic SiO₂ Coatings Produced by Sol-Gel Method

Bożena Pietrzyk ^{*}, Katarzyna Porębska, Witold Jakubowski and Sebastian Mischczak 

Institute of Materials Science and Engineering, Faculty of Mechanical Engineering, Lodz University of Technology, Stefanowskiego Str. 1/15, 90-924 Lodz, Poland; katka.porebska@gmail.com (K.P.); witold.jakubowski@p.lodz.pl (W.J.); sebastian.mischczak@p.lodz.pl (S.M.)

* Correspondence: bozena.pietrzyk@p.lodz.pl; Tel.: +48-42-6313043

Received: 6 May 2019; Accepted: 29 May 2019; Published: 1 June 2019



Abstract: Bacteria existing on the surfaces of various materials can be both a source of infection and an obstacle to the proper functioning of structures. Increased resistance to colonization by microorganisms can be obtained by applying antibacterial coatings. This paper describes the influence of surface wettability and amount of antibacterial additive (Zn) on bacteria settlement on modified SiO₂-based coatings. The coatings were made by sol-gel method. The sols were prepared on the basis of tetraethoxysilane (TEOS), modified with methyltrimethoxysilane (MTMS), hexamethyldisilazane (HMDS) and the addition of zinc nitrate or zinc acetate. Roughness and surface wettability tests, as well as study of the chemical structure of the coatings were carried out. The antibacterial properties of the coatings were checked by examining their susceptibility to colonization by *Escherichia coli*. It was found that the addition of zinc compound reduced the susceptibility to colonization by *E. coli*, while in the studied range, roughness and hydrophobicity did not affect the level of bacteria adhesion to the coatings.

Keywords: SiO₂ coatings; sol-gel; Zn doping; antibacterial coatings; hydrophobic coatings; wettability

1. Introduction

The presence and spread of pathogenic microorganisms in our environment is still a present and growing problem. This problem is exacerbated by the development of microbial resistance to antibiotics and disinfectants. Among the many ways of spreading microorganisms, one of the most widespread is their transfer through tactile contact, in particular through all solid surfaces [1]. Microorganisms living on the touch surfaces can transfer onto the human body during interaction and contribute to the spread of infections [2]. One of the preconditions for the presence of microorganisms on the surfaces of materials is their ability to adhere, which allows the colonization of the surface and the development of a bacterial biofilm [3,4], that is, a source of potential infection associated with the use of materials [5,6]. In addition, microorganisms colonizing surfaces of materials may change their functionality and structure, and even cause degradation (biocorrosion phenomenon) [7].

There are different concepts and strategies for providing antibacterial properties of surfaces [8,9]. These properties, especially increased resistance to colonization and multiplication by bacteria, can be obtained by modifying the surface layer of the material [1,10–12] or by depositing antibacterial coatings with appropriate chemical and physical properties [13–16]. Particularly important, along with free surface energy and surface charge [3,4,17], are hydrophobic properties of the surface, preventing bacterial adhesion and precluding their multiplication. Very important is the degree of surface hydrophobicity [17] and the hydrophobic or hydrophilic properties of the cell walls of the bacteria themselves [18]. The more hydrophobic cells adhere more strongly to hydrophobic surfaces, while hydrophilic cells strongly adhere to hydrophilic surfaces [18]. Insufficient hydrophobicity of the surface,

combined with the hydrophobicity of the bacteria, can increase the propensity of microorganisms to adhesion [17].

The solution, consisting in the production of a coating with antimicrobial properties, is a widely studied and frequently applied approach [13,14,19]. A particularly interesting method for producing such coatings can be the sol-gel method, which makes it possible to produce ceramic oxide coatings from the liquid phase in simple and convenient ways and at a relatively low temperature [20]. Colloidal solution, from which coatings are deposited in this method, allows the easy introduction of a wide spectrum of substances modifying the properties of the resulting thin oxide films, such as in terms of bactericidal activity [21–23]. In order to obtain anti-bacterial properties of such coatings, in addition to providing an appropriate surface wettability condition, it is possible to use the antibacterial properties of metal additives, such as Ag [24–26], Zn [21,27] or Cu [27,28], among others [29]. The impact of metals on bacteria, though widely described and proven [24,30–32], is very diverse and not fully understood, as it is most likely a combination of many different mechanisms [33,34].

The combination of the bactericidal effect of metal ions with the hydrophobicity of the surface of the coating can provide an antibacterial effect through the synergy of both phenomena.

In this work, studies of SiO₂ coatings prepared by sol-gel method, with additions of hydrophobizing compounds and zinc compounds, were carried out. The aim was to determine the impact of these additives on the structure and properties of SiO₂ coatings, in particular, on their antibacterial properties against *Escherichia coli*—understood as limiting the susceptibility of the coatings to colonization and survival of bacteria on their surfaces.

2. Materials and Methods

2.1. Preparation of Sols and Deposition of Coatings

A precursor for the preparation of sols was tetraethoxysilane (TEOS) and Si(OC₂H₅)₄ (98% Fluka). In this study, three types of sols were used: basic SiO₂ sol and two sols of SiO₂ modified with additives, increasing the hydrophobicity of coatings made from these sols. In order to increase hydrophobicity, the additives of methyltrimethoxysilane (MTMS), CH₃Si(OCH₃)₃ (98%, Aldrich) and hexamethyldisilazane (HMDS) HN[Si(CH₃)₃]₂ (98%, Fluka) were used.

The SiO₂ basic sol (sol S) was prepared by dissolving the precursor (TEOS) in anhydrous ethyl alcohol (EtOH) and adding 36% hydrochloric acid (HCl) as a catalyst. The molar ratios of TEOS/EtOH/HCl components were 1:20:0.6.

The sol labeled as M was obtained by adding to the sol S methyltrimethoxysilane (MTMS) so that the molar ratio of TEOS/MTMS was 1:0.64.

The third type of sol was obtained in two stages. In the first stage, the precursor (TEOS) was dissolved in anhydrous ethyl alcohol (EtOH) and 25% NH₄OH was added as the catalyst. The TEOS/EtOH/NH₄OH molar ratios were 1:20:0.1. Then, hexamethyldisilazane (HMDS) was added to the above mixture. The TEOS/HMDS molar ratio was 1:0.5. The second step was mixing the prepared liquid with the same volume of sol M (with the addition of MTMS). In the sol thus prepared, the MTMS/HMDS molar ratio was 1.28:1. This sol was labeled as MH.

After preparing the sols MH and M (hydrophobically modified) the amount of solvent (EtOH) was doubled to give the molar ratio TEOS/EtOH 1:40 to ensure a longer life (extended gelation time in the vessel) of these sols.

Zinc nitrate Zn(NO₃)₂·6H₂O (98%, Chempur) was used as additive for each type of prepared sol in a molar ratio of TEOS/Zn = 1:0.01, 1:0.05 and 1:0.1. After the addition of zinc nitrate, the sol was stirred continuously using a magnetic stirrer (Wigo, Piastów, Poland) for about 10 h at room temperature.

In addition, in order to compare the properties of the coatings doped with Zn derived from different chemical compounds, zinc acetate Zn(CH₃COO)₂·2H₂O (98%, Chempur), was used instead of zinc nitrate additive to the sol M. The molar ratio of TEOS/Zn was preserved and was 1:0.01, 1:0.05 and

1:0.1. After the addition of zinc acetate, the sol was stirred for 2 h at 60°C (to accelerate the dissolution of Zn compound), then 8 h at room temperature.

The priority of choosing the amount of additives was the balance between obtaining the properties of hydrophobic coatings and preserving the stability of the sol as well as the possibility of dissolving the appropriate amount of Zn compounds in the sol. The sols obtained in the manner described above remained stable (i.e., they did not show a tendency to gelate in the vessel or a distinct change in viscosity) for several months.

The labeling of the prepared sols and the chemical compounds used to prepare them are shown in Table 1.

Table 1. Labeling of prepared sols.

Sol Label	Precursor	Hydrophobizer	Zinc Compound	Molar Ratio Si/Zn
S	TEOS	–	–	–
M	TEOS	MTMS	–	–
MH	TEOS	MTMS + HMDS	–	–
SZn1	TEOS	–	Zinc nitrate	0.01
SZn5	TEOS	–	Zinc nitrate	0.05
SZn10	TEOS	–	Zinc nitrate	0.1
MZn1	TEOS	MTMS	Zinc nitrate	0.01
MZn5	TEOS	MTMS	Zinc nitrate	0.05
MZn10	TEOS	MTMS	Zinc nitrate	0.1
MHZn1	TEOS	MTMS+HMDS	Zinc nitrate	0.01
MHZn5	TEOS	MTMS+HMDS	Zinc nitrate	0.05
MHZn10	TEOS	MTMS+HMDS	Zinc nitrate	0.1
MaZn1	TEOS	MTMS	Zinc acetate	0.01
MaZn5	TEOS	MTMS	Zinc acetate	0.5
MaZn10	TEOS	MTMS	Zinc acetate	0.1

Prior to the deposition of coatings, the sols were aged at room temperature for 7 days. The coatings were applied to basic laboratory glass slides with a thickness of 1 mm, as well as on wafers of monocrystalline silicon with an orientation (100) and thickness of 0.3 mm. The surface of the substrates was about 2 cm². Before the deposition process, the substrates were washed in an ultrasonic washer (SONIC-3, Polsonic, Warszawa, Poland) in ethyl alcohol and dried with a stream of compressed air.

Coatings were deposited by dip-coating method using dip-coater (TLO 0.1, MTI Corporation, Richmond, CA, USA), by immersing the substrate in a sol and then withdrawing it at a constant rate of 0.2 mm/s. After applying the coating it was dried at room temperature.

2.2. Characterization of Coatings

The evaluation of coating morphology was carried out using optical microscopy (MO) (MM100, Optatech, Warszawa, Poland) and scanning electron microscopy (SEM) (S-3000M, Hitachi, Tokyo, Japan). Magnifications, 200× (MO) for coatings deposited on glass and silicon substrates and 1000× (SEM) for coatings deposited on a silicon substrates, were applied.

Surface topography of chosen coatings deposited on silicon substrate were measured using atomic force microscope (AFM) (MULTIMODE 5, Bruker Corporation, Billerica, MA, USA) working in tapping mode. All investigations were performed under ambient conditions. Image acquisition was performed with the use of Nanoscope 7.3 software and further image processing was done using Nanoscope Analysis 1.5 software (Bruker Corporation). For each sample, the area of 10 × 10 μm² was scanned. From topography images, commonly used roughness parameters were determined (average values taken from 512 surface profiles).

The thickness of the coatings deposited on silicon substrates was determined using X-ray reflectometry by measuring the intensity of the X-ray beam reflected from the surface of the sample. The tests were carried out using an X-ray diffractometer (EMPYREAN, Malvern Panalytical, Worcestershire,

UK) using characteristic CoK α (1,7903 Å) radiation. Measurements were carried out in the parallel beam geometry in the omega–2theta angle range of 0.1 to 3 degrees. The value of the critical incidence angle was 0.19–0.21 degrees.

The contact angle, defined as the angle formed between the surface on which the drop of water has been deposited and the surface tangent to the drop at the point of contact with the surface, was determined using the drop shape analyzer (DSA100, Kruss GmbH, Hamburg, Germany). The measurements were carried out for coatings deposited on glass substrates.

The chemical structure of the coatings was studied using an Fourier-transform infrared (FTIR) spectrometer (Nicolet iS50, Thermo Fisher Scientific, Waltham, MA, USA) in the range of 4000–400 cm⁻¹. The study was carried out in transmission mode, recording the absorbance of IR radiation passing through coatings deposited on silicon.

2.3. Antibacterial Properties

2.3.1. Bacterial Colonization

The susceptibility to bacterial colonization of *Escherichia coli* (strain DH5 α) was examined on coatings deposited on glass substrates. Directly before the test, the samples were sterilized in water vapor at 121 °C for 20 minutes using a Prestige Medical autoclave. Samples were placed each into a separate flask and immersed in the media containing NaCl (1%), bactopectone (1%) and yeast extract (0.5%), pH = 7.0. The medium was supplemented with a small number (2×10^3) of *E. coli* cells. The samples were incubated for 24 h at 37 °C. After incubation, sample surfaces were extensively washed with deionized water and gently dried. Next, the solution of fluorescent dyes for the visualization of *E. coli* cells was applied to the surface of sample [35].

2.3.2. Visualization of *E. coli* Cells at the Sample Surface

E. coli cells were observed using fluorescence microscope inspection after the application of bis-benzidine and propidium iodide, making the visualization of both live and dead cells possible.

Each surface was robed with the dyes by applying 10 μ L of stock solution of each dyes (100 μ g/mL). The dyes were allowed to penetrate the cells and to bind to dsDNA. This process was carried out for 5 minutes at 28 °C in the dark. Finally, bacterial cells present on the sample surface were detected with the usage of the fluorescence microscope (Olympus GX71) and photos were taken with a CCD camera (DC73). Results for six randomly selected separate areas were inspected for each sample. Image acquisition was carried out using the analySIS DOCU software while counting bacteria using the ImageJ software with plugin "cell counter".

The numbers of killed and surviving bacteria cells were determined for each coating, uncoated glass and uncoated stainless steel 316L, which was used as a reference in each experiment. The number of observed bacteria in each case was related to the control and was presented as a percentage of the control, i.e., the percentage of the number of bacteria on the steel control substrate. At the same time, the level of toxicity of coatings for bacterial cells was demonstrated by calculating the percentage of living cells in relation to all present cells on the tested surface—thanks to the use of live/dead fluorescence staining.

The obtained results were calculated as the mean \pm standard deviation of the test. The presented results contain averaged values of test results for each of the type of coatings.

The tests were carried out for at least four coatings of each type—one or two coatings from at least three series. The series of coatings refers to coatings of the same type produced in a separate experiment. The series of coatings were produced every few weeks under the same laboratory conditions.

3. Results and Discussion

3.1. Characteristics of Coatings

3.1.1. Microscopic Study

During microscopic examination, it was found that the produced coatings were homogeneous, smooth and without cracks and discontinuities. Only in the case of MH coatings with the addition of zinc nitrate, a small number of fine precipitations (visible in the small, limited areas) were observed.

3.1.2. Thickness of Coatings

Thicknesses were determined for coatings made from S, M and MH sols and their counterparts with the addition of zinc compound in the highest amount used (Zn10). The coatings made from unmodified sol had a thickness of about 64 nm (S—67 nm; SZn10—61 nm). The thickness of the coatings obtained from M and MH modified sols was lower—about 22 nm (M—21 nm, MZn10—27 nm, MH—24 nm, MHZn10—18 nm). This is the result of a lower concentration of precursors in these sols.

3.1.3. Topography and Roughness of Coatings

The topography and surface roughness examinations were carried out for coatings made from S, M, MH and SZn10, MZn10, MHZn10 sols, produced on silicon substrates. The results of the roughness measurements are presented in Figure 1.

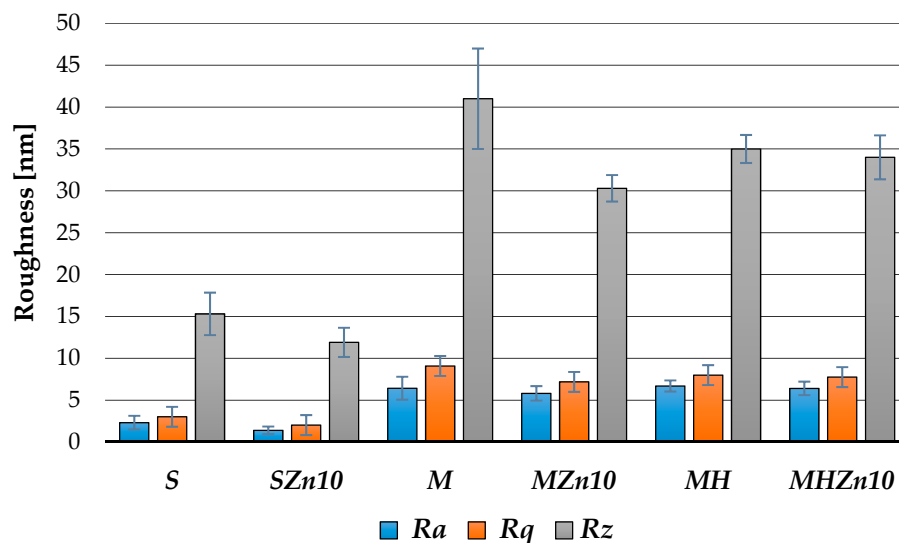


Figure 1. Roughness of coatings with and without Zn additive.

It was found that the modification of coatings using MTMS (M sol) as well as MTMS and HMDS (MH sol) raised the surface roughness compared with unmodified (S) coatings. On the other hand, there was no noticeable change in roughness of coatings with the addition of Zn compared with their Zn-free counterparts. However, it should be noted that despite roughness differences, R_a , R_q and R_z parameters for all of the coatings were very low: $R_a = 1.4\text{--}6.7$ nm; $R_q = 2.0\text{--}9.1$ nm; $R_z = 12\text{--}41$ nm.

The surface topography of S and SZn10, as well as MH and MHZn10 coatings, is shown in Figure 2. Similarly, as in the case of roughness parameters, there was a pronounced difference between coatings made from S and MH sols, while surface topographies of Zn doped and corresponding non-doped coatings (S vs. SZn10 and MH vs. MHZn10) were similar.

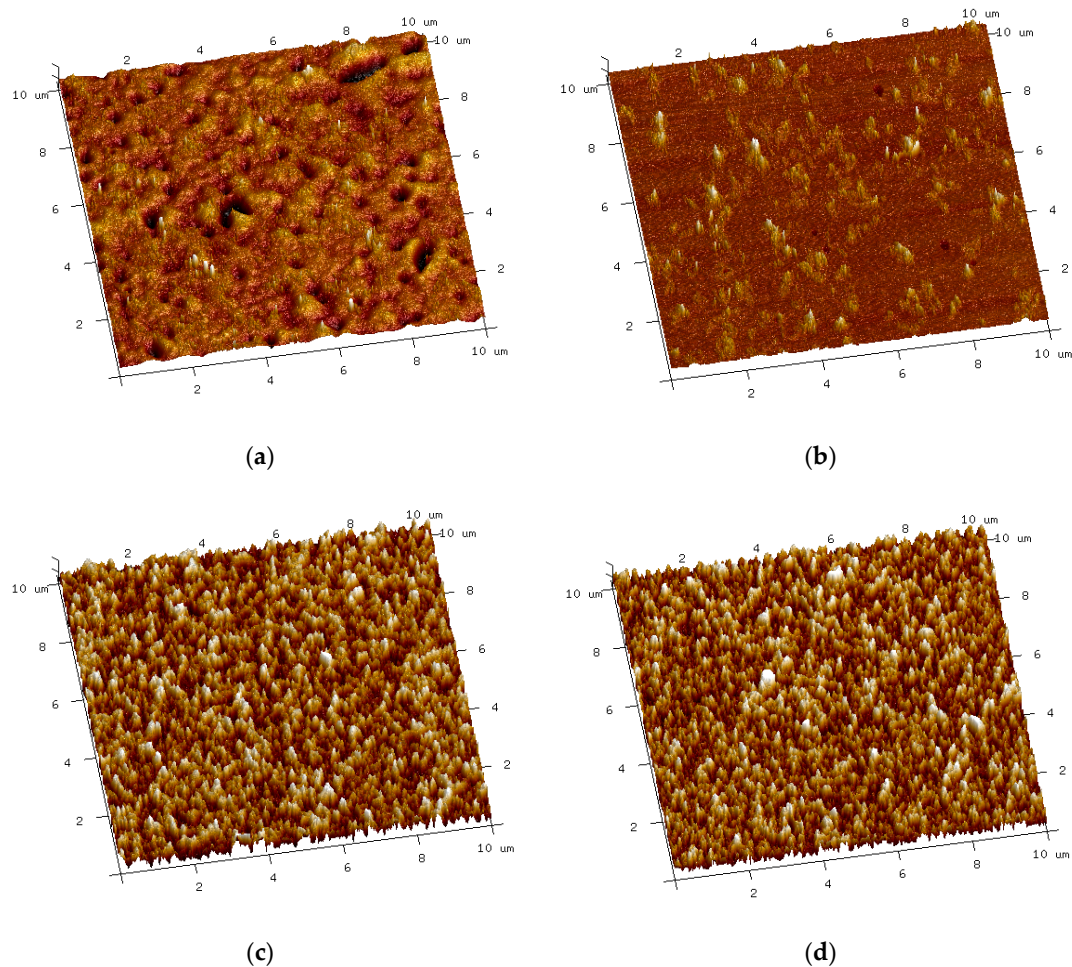


Figure 2. Topography of coatings: (a) SiO_2 (sol S) coating; (b) SiO_2+Zn (sol SZn10) coating; (c) Modified SiO_2 coating (sol MH); (d) Modified SiO_2+Zn coating (sol MHZn10).

3.1.4. Wettability of Coatings

In order to evaluate the results of coatings modifications with hydrophobic additives (MTMS and HMDS), the measurements of surface contact angles were performed. The results are shown in Figure 3.

The contact angles of coatings deposited from unmodified S sols were between 40° and 46° and were higher than the contact angle of the surface of untreated glass (30°). The modification of sols using hydrophobizers had a significant effect on the level of surface wettability. For coatings prepared from M sols, the contact angle was about 90° – 95° . The highest level of hydrophobicity was obtained for coatings prepared from MH sol and was 102° . Figure 3 shows that the Zn additive does not significantly affect the wettability of coatings—differences of contact angles for the same type of sol with various Zn content are very small.

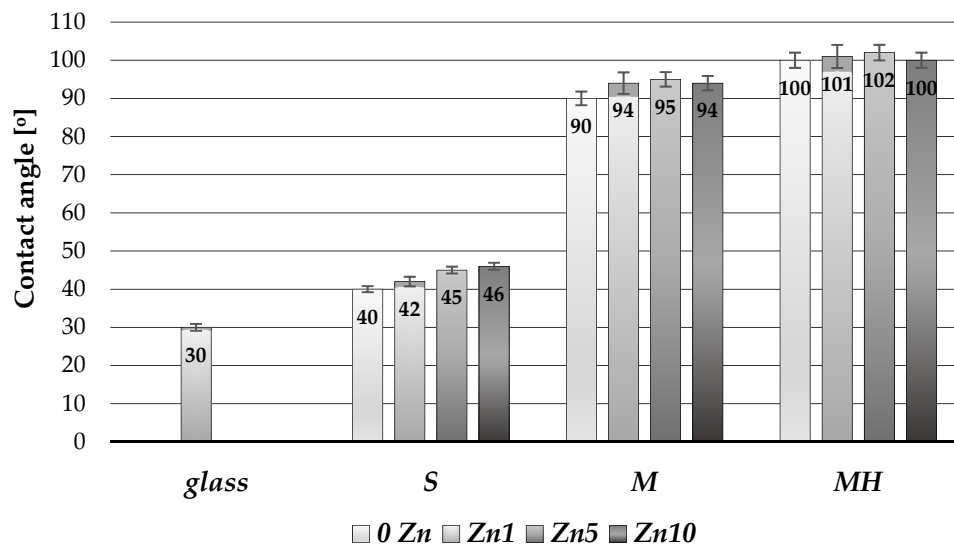


Figure 3. Wettability of coatings.

3.1.5. Chemical Structure of Coatings

The chemical structure of the coatings was analyzed using FTIR infrared spectroscopy for all types of coatings without the addition of Zn (S, M, MH) and with the addition of zinc nitrate in the highest applied amount (SZn10, MZn10, MHZn10). Exemplary FTIR spectra of coatings are presented in Figures 4–6.

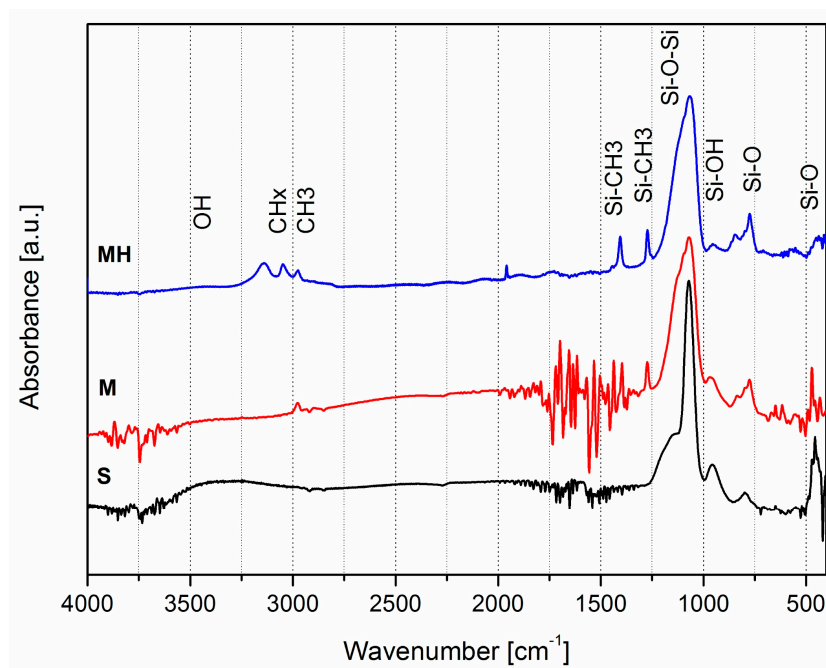


Figure 4. FTIR spectra of coatings obtained from sols S, M and MH.

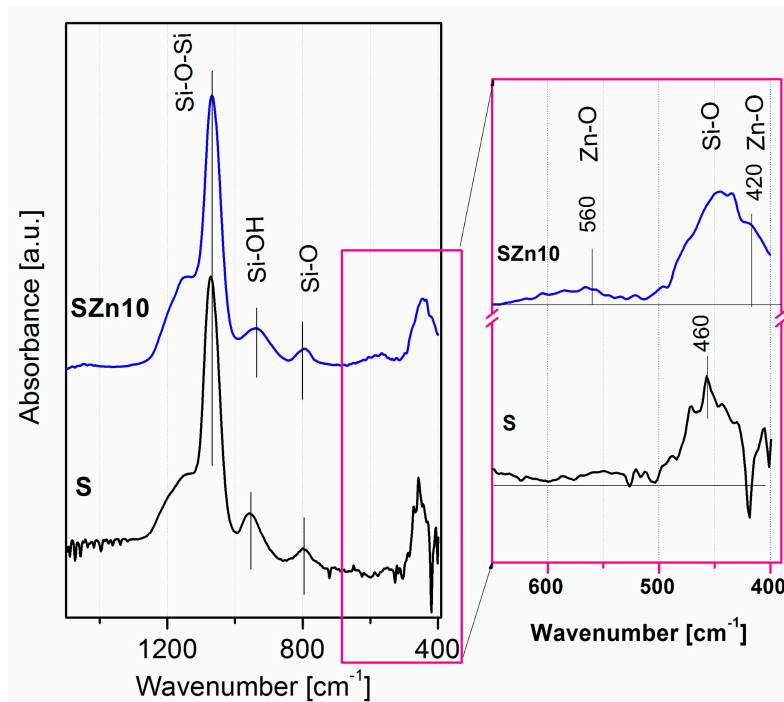


Figure 5. FTIR spectra of S and SZn10 coatings.

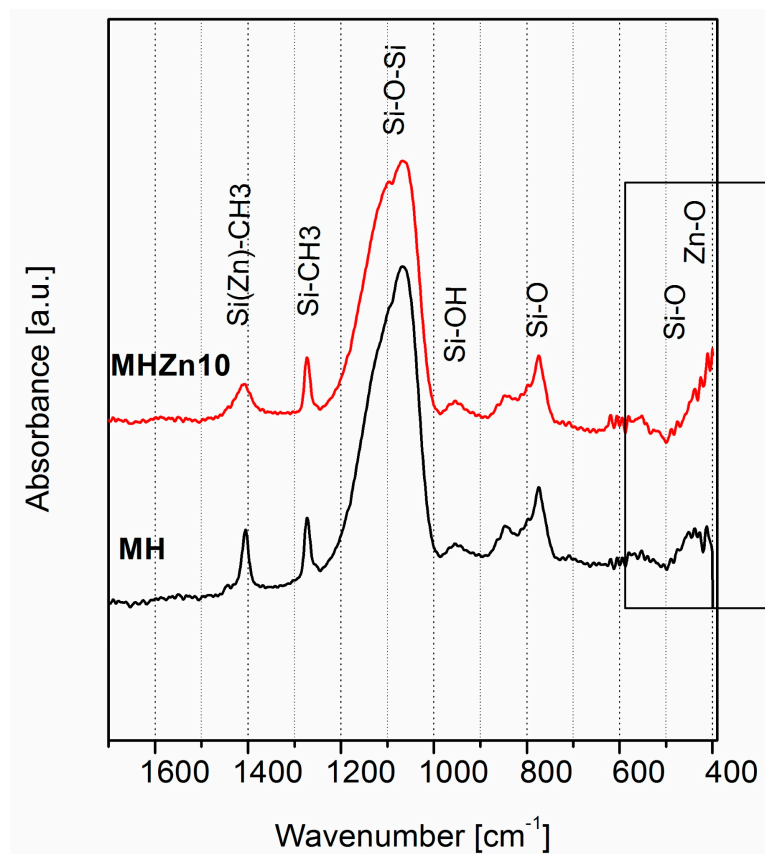


Figure 6. FTIR spectra of MH and MHZn10 coatings.

In the spectra of coatings S, M and MH shown in Figure 4, absorption bands typical for SiO₂ were observed: 460, 800, 1095 cm⁻¹, respectively. In the range of 3000–3500 cm⁻¹, in the spectrum of the S coating, a broad band typical of hydroxyl bonds was visible. In the spectra of coatings M and MH,

absorption bands resulting from the presence of methyl groups $-\text{CH}_3$ for 1274 and 2970 cm^{-1} were also visible in the coating structure. Moreover, in the spectrum of the coating MH, bands were also observed from these groups of about 1400 cm^{-1} and in the range of $2970\text{--}3100\text{ cm}^{-1}$. In the spectra of M and MH coatings, the amount of hydroxyl groups (ranging from $3000\text{--}3500\text{ cm}^{-1}$) was reduced as the amount of methyl groups increased. The presence of methyl groups in M and MH coatings was responsible for lowering their wettability (increase of contact angle) [36,37].

Changes in the chemical structure caused by Zn doping of the SiO_2 coating are shown in Figure 5. They were visible in the range of $400\text{--}600\text{ cm}^{-1}$, characteristic for Zn–O bonds. They consisted in the appearance of an additional band of 420 cm^{-1} and a weak band of 560 cm^{-1} in the spectrum of the coating with the addition of Zn compared with the spectrum of the undoped coating.

In the spectra of hydrophobized coatings M and MH, the changes caused by the addition of zinc nitrate were analogous to those obtained from the S sol. These changes are visible within the marked fragment in Figure 6 showing the FTIR spectra of the MH and MHZn10 coatings. Additionally, in the FTIR spectrum of MHZn10 coating, the widening of the 1415 cm^{-1} band was observed, which may indicate the replacement of the Si atom by Zn in the Si– CH_3 connections [38]. The analysis of the spectra shown in Figures 5 and 6 demonstrate that the zinc atoms were bound in the coating by a chemical bond with oxygen (Zn–O) as well as in the Si(Zn)– CH_3 bonds.

3.2. Antibacterial Properties of the Coatings

The results of testing the susceptibility of the surface on microbial colonization and survival of the bacteria on the surfaces of the coatings deposited on glass substrates are shown in Figures 7 and 8. The results of bacterial adhesion testing are presented as the number of bacteria on the tested surface with respect to the number of bacteria on the surface of the steel control sample (% of control). The survival rate of the bacteria are presented as a percentage share of the bacteria living among all the bacteria present on the surface.

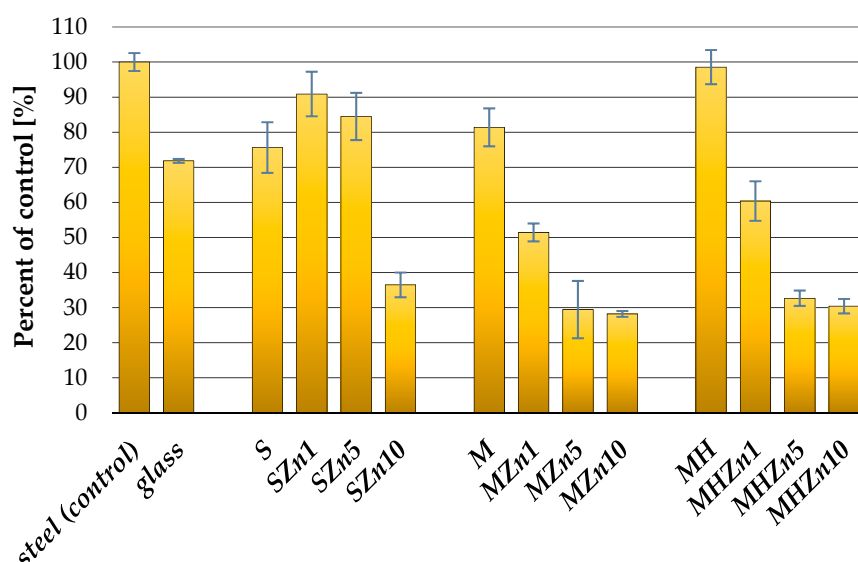


Figure 7. The colonization of bacteria on tested surfaces.

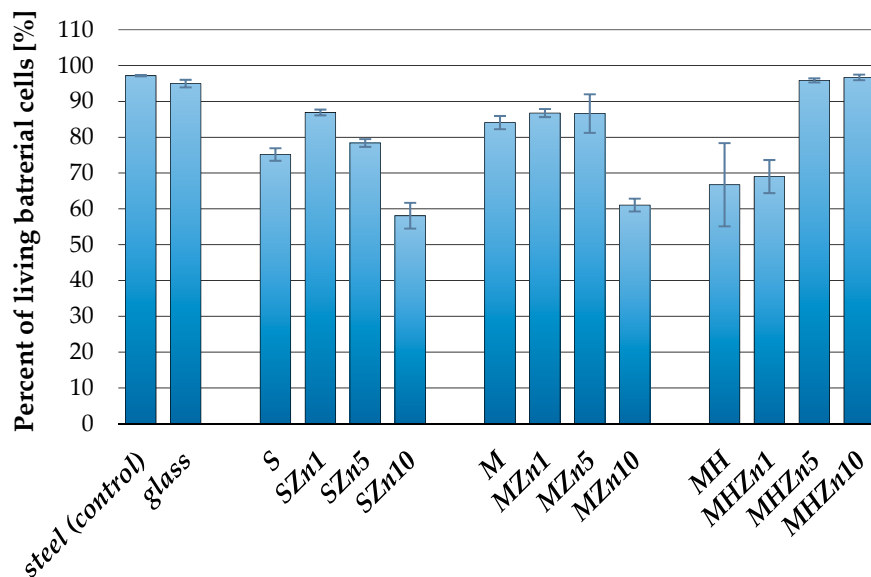


Figure 8. Survivability of bacteria on tested surfaces.

Based on the results shown in Figure 7, it can be concluded that the addition of zinc reduces the degree of surface colonization by *E. coli* bacteria, reducing the amount of bacteria colonizing the surfaces of the coatings compared with those without the addition of Zn. The effect of reducing the number of bacteria adhered to the surface was observed on all types of coatings with the addition of zinc (SZn, MZn and MHZn). For each type of coating, the number of bacteria bound to the surface decreased with the increase in the amount of added zinc.

The best antibacterial effects were obtained for coatings with the maximum amount of used additive Zn10. For all types of coatings doped with zinc Zn10, the number of bacteria was about 30% of the number of bacteria adhered to the surface of the steel control sample.

At the same time, there was no relationship between the survivability of bacteria on the tested surfaces and the type of coating (Figure 8). It can only be concluded that the number of living bacteria *E. coli* on the surface of the coatings was lower than on substrates without coating (steel, glass).

The percentage of living bacteria on the coatings was 60%–85% of the control, with the exception of coatings MHZn5 and MHZn10, where it was comparable to the control surface. However, the conducted studies do not show a clear correlation between the reduction in bacterial survivability and the type of hydrophobic modification or the content of zinc.

In order to determine the influence of zinc addition on coating properties, the properties of coatings doped with various zinc compounds were compared: nitrate $Zn(NO_3)_2$ and acetate $Zn(CH_3CO_2)_2$. Results of colonization and bacterial survivability studies on M type coatings doped by different Zn compounds are presented in Figure 9.

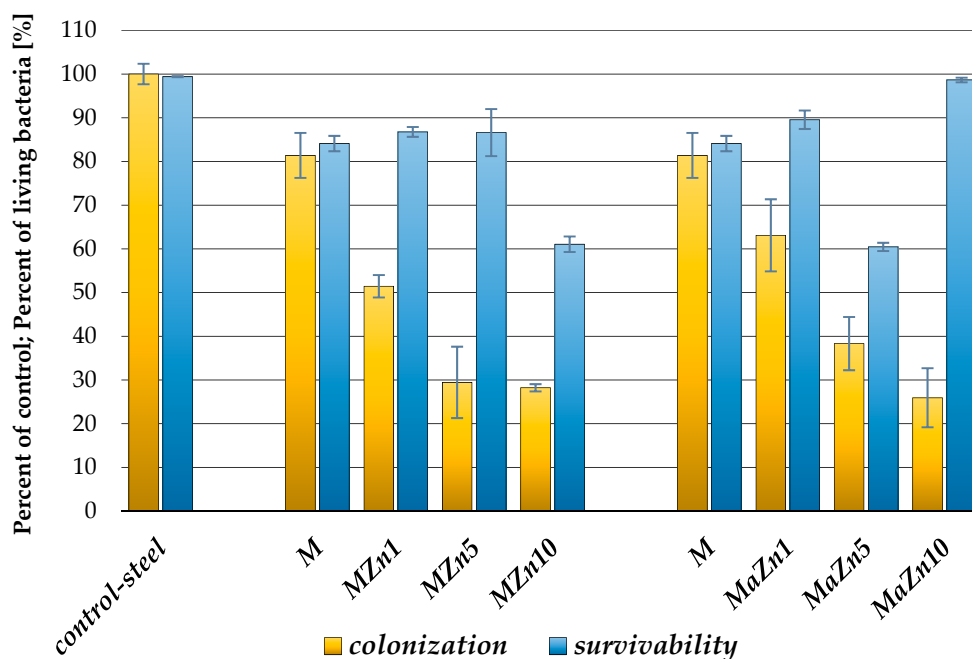


Figure 9. Comparison of antibacterial properties of M type coatings doped by different Zn compounds: nitrate (MZn1, MZn5, MZn10) and acetate (MaZn1, MaZn5, MaZn10).

The antibacterial properties of the tested coatings were similar regardless of the type of compound used to introduce Zn into the coating. For both types of Zn compound, with the increase in its content, the susceptibility to colonization of *E. coli* decreased to less than 30% relative to the control surface (stainless steel), while the survivability of the bacteria did not show a clear tendency with the change of the Zn additive amount.

4. Summary and Conclusions

This paper presents research on topography, surface wettability, chemical structure and level of colonization by *E. coli* of SiO₂ coatings modified with hydrophobizing additives and zinc compounds.

Obtained coatings were homogeneous and smooth (without significant defects or discontinuities) and were not damaged (cracks or detachments from the substrate) after the sterilization processes. No correlation was observed between the coating's roughness and its antibacterial properties. Changes in roughness as a result of the performed modifications were too small ($Ra = 1.4\text{--}6.7$ nm, $Rq = 2.0\text{--}9.1$ nm) to have had a significant effect on bacterial behavior [39].

Coatings showed differences in microscopic surface topography and surface wettability as a result of their modification with hydrophobizers (MTMS and HMDS). Changes in wettability of unmodified and MTMS/HMDS modified coatings resulted from the introduction of $-\text{CH}_3$ (methyl) groups into the coating structure. It was found that MTMS/HMDS-modified coatings showed an increase in hydrophobicity, but the extent of this change was not sufficient enough to significantly reduce the adhesion of *E. coli*. This coincides with literature reports in which the effect of the smaller contact angles in the hydrophobic range on the ability to settle the bacteria is not clear [40,41] and only the achievement of very high wetting angles (above 150°) provides a pronounced resistance to colonization [17].

A factor that had a significant impact on the antibacterial properties of the coatings was the additive of zinc. With the increase of Zn content, the susceptibility of the surface to colonization by *E. coli* decreased regardless of the type of compound used to introduce Zn into the coating. Investigations of the chemical structure of the coatings showed that the Zn atoms (introduced into the silica sol in the

form of salts) were incorporated into the coating structure by chemical bonds with oxygen (Zn–O) and alkyl groups, which ensured its antibacterial properties.

A summary of data on wettability and colonization of *E. coli* on the surfaces of all types of coatings without Zn additive and with the highest concentration of doped Zn is shown in Figure 10.

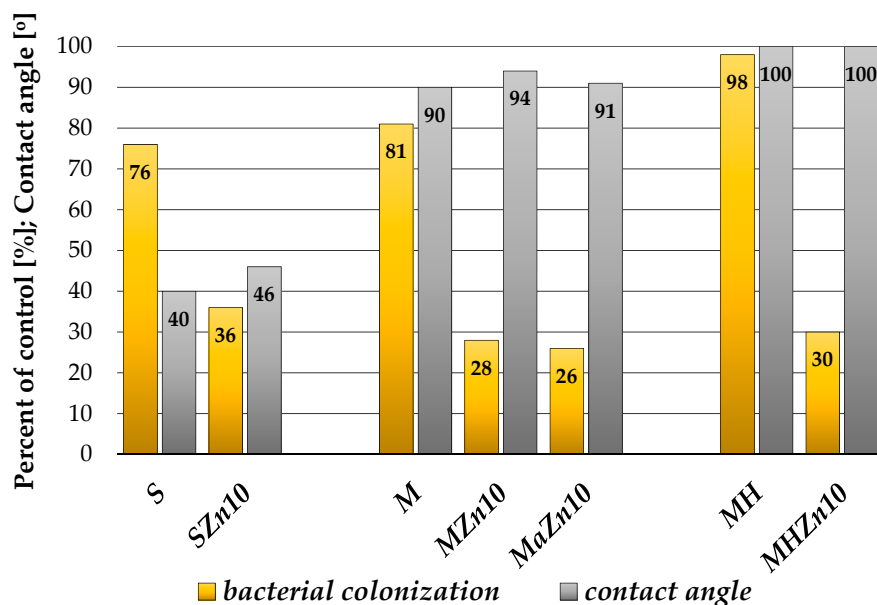


Figure 10. Comparison of mean wettability of the coatings and their colonization by *E. coli*.

Another studied feature of the coatings was the survival rate of the adhered bacteria, which can be treated as a measure of surface toxicity against microorganisms. The conducted research showed no statistically significant effect of any of the studied factors on the survival of *E. coli* bacteria already settled on the surface. Figure 8 shows that the share of living bacteria among the bacteria inhabiting the surface of the coating was slightly lower than that for the control surfaces, but no trend can be pointed out in this respect. This result, however, indicates a beneficial mechanism of antibacterial activity of Zn doped coatings, which reduce the number of bacteria colonizing the surface more than only contributing to their death. In the absence of the reduction of colonization intensity on the surface, dead bacteria would create a layer isolating newly settled cells from the coating containing an antibacterial agent, which would promote the formation of a bacterial biofilm [3,42]. Prevention of bacterial biofilm formation, observed in the case of Zn doped coatings, is a key feature of antibacterial touch surfaces [1,6,43].

The conducted research allows us to conclude that examined coatings show antimicrobial activity by limiting their colonization by bacteria (*E. coli*). The obtained effect is a result of the use of Zn additive in the coatings, not due to the hydrophobic properties of their surface (Figure 10). Therefore, the expected synergy of hydrophobicity and Zn doping in terms of antibacterial activity was not found.

The simple and convenient way of coatings produced using the sol-gel method, with a low thickness and manufacturing process which takes place entirely at room temperature, enables their potential application as antibacterial coatings on many types of substrates.

Author Contributions: P.B.: Concept, Methodology, Investigations, Results Analysis, Writing, Editing and Supervising the Manuscript; P.K.: Methodology, Investigations, Data and Results Analysis; J.W.: Biological Investigations, Data Analysis, Discussion; M.S.: Results Analysis, Discussion, Writing and Editing the Manuscript.

Funding: This research received no external funding.

Acknowledgments: The authors acknowledge Anna Sobczyk-Guzenda for recording of FTIR spectra and Łukasz Kołodziejczyk for obtaining AFM images.

Conflicts of Interest: The authors declare no conflict of interest.

References

1. Villapún, V.M.; Dover, L.G.; Cross, A.; González, S. Antibacterial metallic touch surfaces. *Materials* **2016**, *9*, 736. [[CrossRef](#)]
2. Page, K.; Wilson, M.; Parkin, I.P. Antimicrobial surfaces and their potential in reducing the role of the inanimate environment in the incidence of hospital-acquired infections. *J. Mater. Chem.* **2009**, *19*, 3819–3831. [[CrossRef](#)]
3. Carniello, V.; Peterson, B.W.; van der Mei, H.C.; Busscher, H.J. Physico-chemistry from initial bacterial adhesion to surface-programmed biofilm growth. *Adv. Colloid Interface Sci.* **2018**, *261*, 1–14. [[CrossRef](#)]
4. Song, F.; Koo, H.; Ren, D. Effects of material properties on bacterial adhesion and biofilm formation. *J. Dent. Res.* **2015**, *94*, 1027–1034. [[CrossRef](#)] [[PubMed](#)]
5. Ramasamy, M.; Lee, J. Recent nanotechnology approaches for prevention and treatment of biofilm-associated infections on medical devices. *BioMed Res. Int.* **2016**, *2016*, 1851242. [[CrossRef](#)] [[PubMed](#)]
6. Jamal, M.; Ahmad, W.; Andleeb, S.; Jalil, F.; Imran, M.; Nawaz, M.A.; Hussain, T.; Ali, M.; Rafiq, M.; Kamil, M.A. Bacterial biofilm and associated infections. *J. Chin. Med. Assoc.* **2018**, *81*, 7–11. [[CrossRef](#)]
7. Kip, N.; van Veen, J.A. The dual role of microbes in corrosion. *ISME J.* **2014**, *9*, 542–551. [[CrossRef](#)] [[PubMed](#)]
8. Campoccia, D.; Montanaro, L.; Arciola, C.R. A review of the biomaterials technologies for infection-resistant surfaces. *Biomaterials* **2013**, *34*, 8533–8554. [[CrossRef](#)] [[PubMed](#)]
9. Sun, D.; Babar Shahzad, M.; Li, M.; Wang, G.; Xu, D. Antimicrobial materials with medical applications. *Mater. Technol.* **2015**, *30*, B90–B95. [[CrossRef](#)]
10. Elbourne, A.; Crawford, R.J.; Ivanova, E.P. Nano-structured antimicrobial surfaces: From nature to synthetic analogues. *J. Colloid Interface Sci.* **2017**, *508*, 603–616. [[CrossRef](#)] [[PubMed](#)]
11. Henriques, P.C.; Borges, I.; Pinto, A.M.; Magalhães, F.D.; Gonçalves, I.C. Fabrication and antimicrobial performance of surfaces integrating graphene-based materials. *Carbon* **2018**, *132*, 709–732. [[CrossRef](#)]
12. Champagne, V.; Sundberg, K.; Helfritsch, D. Kinetically deposited copper antimicrobial surfaces. *Coatings* **2019**, *9*, 257. [[CrossRef](#)]
13. Swartjes, J.J.T.M.; Sharma, P.K.; van Kooten, T.G.; van der Mei, H.C.; Mahmoudi, M.; Busscher, H.J.; Rochford, E.T.J. Current developments in antimicrobial surface coatings for biomedical applications. *Curr. Med. Chem.* **2015**, *22*, 2116–2129. [[CrossRef](#)] [[PubMed](#)]
14. Cloutier, M.; Mantovani, D.; Rosei, F. Antibacterial coatings: Challenges, perspectives, and opportunities. *Trends Biotechnol.* **2015**, *33*, 637–652. [[CrossRef](#)] [[PubMed](#)]
15. Adlhart, C.; Verran, J.; Azevedo, N.F.; Olmez, H.; Keinänen-Toivola, M.M.; Gouveia, I.; Melo, L.F.; Crijns, F. Surface modifications for antimicrobial effects in the healthcare setting: a critical overview. *J. Hosp. Infection* **2018**, *99*, 239–249. [[CrossRef](#)]
16. Li, R.; Jin, Z.T.; Liu, Z.; Liu, L. Antimicrobial double-layer coating prepared from pure or doped-titanium dioxide and binders. *Coatings* **2018**, *8*, 41. [[CrossRef](#)]
17. Zhang, X.; Wang, L.; Levänen, E. Superhydrophobic surfaces for the reduction of bacterial adhesion. *RSC Adv.* **2013**, *3*, 12003–12020. [[CrossRef](#)]
18. Krasowska, A.; Sigler, K. How microorganisms use hydrophobicity and what does this mean for human needs? *Front. Cell. Infect. Microbiol.* **2014**, *4*, 112. [[CrossRef](#)] [[PubMed](#)]
19. Salwiczek, M.; Qu, Y.; Gardiner, J.; Strugnell, R.A.; Lithgow, T.; McLean, K.M.; Thissen, H. Emerging rules for effective antimicrobial coatings. *Trends Biotechnol.* **2014**, *32*, 82–90. [[CrossRef](#)] [[PubMed](#)]
20. Levy, D.; Zayat, M. *The Sol-Gel Handbook: Synthesis, Characterization and Applications*, 1st ed.; Wiley-VCH Verlag GmbH & Co. KGaA: Weinheim, Germany, 2015.
21. Jaiswal, S.; McHale, P.; Duffy, B. Preparation and rapid analysis of antibacterial silver, copper and zinc doped sol-gel surfaces. *Colloids Surf. B Biointerfaces* **2012**, *94*, 170–176. [[CrossRef](#)]
22. Owens, G.J.; Singh, R.K.; Foroutan, F.; Alqaysi, M.; Han, C.-M.; Mahapatra, C.; Kim, H.-W.; Knowles, J.C. Sol-gel based materials for biomedical applications. *Prog. Mater. Sci.* **2016**, *77*, 1–79. [[CrossRef](#)]
23. Khokhlova, M.; Dykas, M.; Krishnan-Kutty, V.; Patra, A.; Venkatesan, T.; Prellier, W. Oxide thin films as bioactive coatings. *J. Phys. Condens. Matt.* **2018**, *31*, 033001. [[CrossRef](#)]
24. Chernousova, S.; Epple, M. Silver as antibacterial agent: Ion, nanoparticle, and metal. *Angew. Chem. Int. Ed.* **2013**, *52*, 1636–1653. [[CrossRef](#)] [[PubMed](#)]

25. Jung, W.K.; Koo, H.C.; Kim, K.W.; Shin, S.; Kim, S.H.; Park, Y.H. Antibacterial activity and mechanism of action of the silver ion in staphylococcus aureus and *Escherichia coli*. *Appl. Environ. Microbiol.* **2008**, *74*, 2171. [[CrossRef](#)] [[PubMed](#)]
26. Jeon, H.-J.; Yi, S.-C.; Oh, S.-G. Preparation and antibacterial effects of Ag-SiO₂ thin films by sol-gel method. *Biomaterials* **2003**, *24*, 4921–4928. [[CrossRef](#)]
27. Jäger, E.; Schmidt, J.; Pfuch, A.; Spange, S.; Beier, O.; Jäger, N.; Jantschner, O.; Daniel, R.; Mitterer, C. Antibacterial silicon oxide thin films doped with zinc and copper grown by atmospheric pressure plasma chemical vapor deposition. *Nanomaterials* **2019**, *9*, 255. [[CrossRef](#)]
28. Trapalis, C.C.; Kokkoris, M.; Perdikakis, G.; Kordas, G. Study of antibacterial composite Cu/SiO₂ thin coatings. *J. Sol-Gel Sci. Technol.* **2003**, *26*, 1213–1218. [[CrossRef](#)]
29. Turner, R.J. Metal-based antimicrobial strategies. *Microb. Biotechnol.* **2017**, *10*, 1062–1065. [[CrossRef](#)] [[PubMed](#)]
30. Kumar, V.V.; Anthony, S.P. Antimicrobial studies of metal and metal oxide nanoparticles. In *Surface Chemistry of Nanobiomaterials*; Grumezescu, A.M., Ed.; William Andrew Publishing: Norwich, NY, USA, 2016; pp. 265–300.
31. Vincent, M.; Hartemann, P.; Engels-Deutsch, M. Antimicrobial applications of copper. *Int. J. Hyg. Environ. Health* **2016**, *219*, 585–591. [[CrossRef](#)] [[PubMed](#)]
32. Pasquet, J.; Chevalier, Y.; Pelletier, J.; Couval, E.; Bouvier, D.; Bolzinger, M.-A. The contribution of zinc ions to the antimicrobial activity of zinc oxide. *Colloids Surf. A Physicochem. Eng. Aspects* **2014**, *457*, 263–274. [[CrossRef](#)]
33. Lemire, J.A.; Harrison, J.J.; Turner, R.J. Antimicrobial activity of metals: mechanisms, molecular targets and applications. *Nat. Rev. Microbiol.* **2013**, *11*, 371. [[CrossRef](#)] [[PubMed](#)]
34. Mittapally, S.; Taranum, R.; Parveen, S. Metal ions as antibacterial agents. *JDDT* **2018**, *8*, 411–419. [[CrossRef](#)]
35. Jakubowski, W.; Bartosz, G.; Niedzielski, P.; Szymanski, W.; Walkowiak, B. Nanocrystalline diamond surface is resistant to bacterial colonization. *Diam. Relat. Mater.* **2004**, *13*, 1761–1763. [[CrossRef](#)]
36. Cai, S.; Zhang, Y.; Zhang, H.; Yan, H.; Lv, H.; Jiang, B. Sol-gel preparation of hydrophobic silica antireflective coatings with low refractive index by base/acid two-step catalysis. *ACS Appl. Mater. Interfaces* **2014**, *6*, 11470–11475. [[CrossRef](#)]
37. Philipavičius, J.; Kazadojev, I.; Beganskienė, A.; Melninkaitis, A.; Sirutkaitis, V.; Kareiva, A. Hydrophobic antireflective silica coatings via sol-gel process. *Mater. Sci.* **2008**, *14*, 283–287.
38. Long, D.A. Infrared and Raman Characteristic Group Frequencies. *Tables and charts George Socrates John Wiley and Sons, Ltd, Chichester, Third Edition, 2001, J. Raman Spectrosc.* **2004**, *35*, 905.
39. Preedy, E.; Perni, S.; Nipič, D.; Bohinc, K.; Prokopovich, P. Surface roughness mediated adhesion forces between borosilicate glass and *Gram-Positive Bacteria*. *Langmuir* **2014**, *30*, 9466–9476. [[CrossRef](#)]
40. Tang, L.; Pillai, S.; Revsbech, N.P.; Schramm, A.; Bischoff, C.; Meyer, R.L. Biofilm retention on surfaces with variable roughness and hydrophobicity. *Biofouling* **2011**, *27*, 111–121. [[CrossRef](#)]
41. Bazaka, K.; Crawford, R.J.; Ivanova, E.P. Do bacteria differentiate between degrees of nanoscale surface roughness? *Biotechnol. J.* **2011**, *6*, 1103–1114. [[CrossRef](#)]
42. Garrett, T.R.; Bhakoo, M.; Zhang, Z. Bacterial adhesion and biofilms on surfaces. *Prog. Nat. Sci.* **2008**, *18*, 1049–1056. [[CrossRef](#)]
43. Bjarnsholt, T. The role of bacterial biofilms in chronic infections. *APMIS* **2013**, *121*, 1–58. [[CrossRef](#)] [[PubMed](#)]

